

X-ray diagnostics for investigating electron distribution functions in the central cell of the GAMMA 10 tandem mirror

J. Kohagura, T. Cho, M. Hirata, T. Numakura, T. Fukai, Y. Tomii, S. Kiminami, N. Morimoto, T. Ikuno, S. Namiki, K. Shimizu, M. Ito, Y. Miyata, R. Minami, and S. Miyoshi

Plasma Research Centre, University of Tsukuba, Ibaraki 305-8577, Japan

K. Ogura

Graduate School of Science and Technology, Niigata University, Niigata 950-2181, Japan

N. Saito and T. Saito

National Institute of Advanced Industrial Science and Technology, Ibaraki 305-8568, Japan

T. Kariya

Toshiba Electron Tubes and Devices, Tochigi 324-8550, Japan

(Received 7 May 2006; presented on 10 May 2006; accepted 14 August 2006; published online 20 October 2006)

The quantum efficiency of an ultralow-energy-sensitive pure-Ge (ULE Ge) detector is investigated using synchrotron radiation from the storage ring at AIST especially for x-ray pulse-height analyses (PHAs), down to a few hundred eV. Several types of x-ray diagnostics such as x-ray PHA, x-ray absorption methods, and x-ray tomography using the ULE Ge detector, a NaI(Tl) detector, as well as a microchannel-plate tomography system are employed for investigating electron distribution functions and electron temperature profiles with preliminary central electron-cyclotron heating in the central cell of the GAMMA 10 tandem mirror. These measurements play an important role in studying an essential physics scaling of the electron temperature as a function of electron confining potential in tandem mirror plasmas. © 2006 American Institute of Physics.

[DOI: [10.1063/1.2351922](https://doi.org/10.1063/1.2351922)]

I. INTRODUCTION

In GAMMA 10,¹⁻³ the second-harmonic electron-cyclotron heating (ECH) in the barrier region (barrier ECH) is utilized for the formation of a thermal-barrier potential ϕ_b , which reduces the electron heat flow between the central cell and the plug region and plays an important role as an electron confining potential in the central cell.¹⁻³

Construction and verification of the physics scaling of the central-cell electron temperature T_e are two of the main issues for tandem mirror plasmas. Recently we have proposed the physics scaling law of T_e as a function of ϕ_b by using the energy balance equation for a central-cell bulk electron energy density and Pastukhov's theory for electron energy confinement time.³⁻⁵ In the central cell of GAMMA 10, heating sources for the bulk electrons are hot ions with temperatures $T_i=1-10$ eV produced by ion-cyclotron heating (ICH) and other higher-temperature electron components coming from other regions.^{4,6} Preliminary application of central ECH which can be another heating source for central-cell electrons is carried out in the present study. Electron temperatures of those components called warm or hot component are in the range from a few keV to a few hundred keV. Due to lack of sufficient direct electron heating sources, typical bulk electron temperature stays in the order of 100 eV. In order to investigate the T_e - ϕ_b scaling it is essential to clarify electron energy distribution functions and electron temperature profiles in such a wide energy range. Here the detection efficiency of an ultralow-energy-sensitive pure-Ge (ULE Ge)

detector⁷ (Canberra GUL0035) is precisely investigated by using synchrotron radiation especially for the observation of x-ray spectrum down to a few hundred eV. The ULE Ge detector, a NaI(Tl) detector,⁶ as well as a microchannel-plate (MCP) tomography system^{8,9} are employed to obtain electron distribution functions including a bulk electron component and electron temperature profiles.⁶⁻⁹

II. GAMMA 10 TANDEM MIRROR AND X-RAY DIAGNOSTIC SYSTEMS

GAMMA 10 is a minimum-B anchored tandem mirror with outboard axisymmetric plug-and-barrier mirror cells for the formation of electrostatic ion-confining potentials ϕ_c and electrostatic thermal-barrier potentials ϕ_b . The central cell has a length of 6 m and a limiter with a diameter of 36 cm, and the magnetic-field intensity at the midplane is 0.405 T with a mirror ratio R_m of 5.2. Ion-cyclotron heatings at 6.3 MHz are employed for producing hot ions. Preliminary central ECH is employed (90 kW at 28 GHz) in the central cell for the present study.

In the central cell several x-ray diagnostic systems⁶ are used including the ULE Ge detector, the NaI(Tl) detector, and the MCP tomography system. Figure 1 shows a schematic view of detector radial locations in one plane for convenience. Their locations in the z direction are +60, +120, and 0 cm, respectively.

The ULE Ge detector is used to measure the energy spectrum ranging from a few hundred eV to a few tens keV.

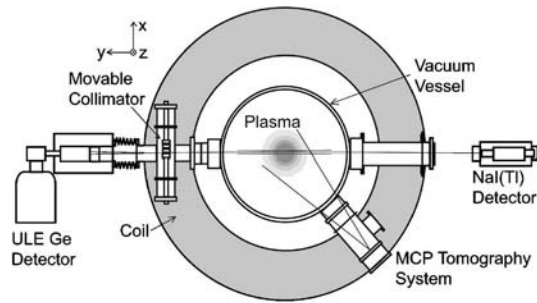


FIG. 1. Schematic drawings of x-ray diagnostic systems in the central cell of GAMMA 10.

The ULE Ge detector retains the high-energy efficiency as well because of the high atomic number and thus covers a wide range of energies up to a few hundred keV. Another pulse-height analysis (PHA) system using the NaI(Tl) detector (5 cm thick, 2.5 cm diameter, with a 2 mm aluminum entrance window) is employed to measure the photon spectrum from 20 to 750 keV.

X-ray brightness is obtained spatially and temporally by the use of a 50-channel MCP system. The system is used to measure bulk electron temperature profiles. Here, we use the detailed calibration data on the MCP as a function of x-ray energy (from 12 eV to 82 keV) and incident angle. The specifications of the MCP are as follows; the channel pore diameter D is 15 μm , the channel pitch is 19 μm , and the channel length L_c is 0.6 mm. The length-to-diameter ratio L_c/D is 40. The channel bias angle θ is 13°. The open-area ratio is 57%. The active area of the MCP is 31 \times 81 mm². This area is divided into 50 sections in line, and each section has an anode to collect secondary electrons intensified in the MCP. The MCP system using a pinhole camera geometry includes an exchangeable photon absorber assembly for x-ray absorption method.

III. CALIBRATION OF AN ULTRALOW-ENERGY MEASURABLE PURE-GERMANIUM DETECTOR

The characterization experiment of the ULE Ge detector is carried out using synchrotron radiation at TERAS of the National Institute of Advanced Industrial Science and Technology (AIST).^{10,11} A 310 MeV injector linear accelerator (LINAC) has been operated and has provided 760 MeV electron beams for the electron storage ring TERAS. The storage current of 100 mA has a lifetime of about 8 h. The storage ring has a circumference of 31.45 m.

Figure 2(a) illustrates the schematic drawings of our experimental setup. The beamline¹⁰ (BL1-A) consists of a premirror, a grasshopper monochromator, a refocusing mirror, a beam monitor, and variable x-ray filters. The photon energy is changed from 0.1 to 1.0 keV by automated control of the grasshopper monochromator. The grating has 2400 grooves/mm, a blaze angle of 1.72°, and a curvature radius of 2 m. The energy resolution of the system is ~ 0.2 eV at 245 eV and ~ 1 eV at 400 eV. Thin filters (Be, Al) are utilized in order to suppress stray and higher-order radiation. An incident photon flux is monitored by photo-

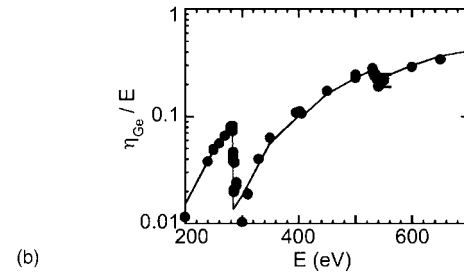
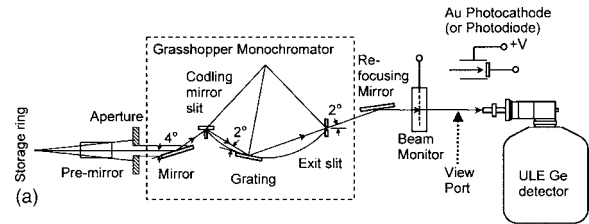


FIG. 2. (a) Schematic drawings of the experimental apparatus in TERAS. (b) The quantum efficiency of the ULE Ge detector normalized by the incident x-ray energy. The theoretical curve (the solid line) is calculated based on the x-ray absorptions by a specially fabricated polymer window.

electric currents (I_0) from a Au-coated Ni mesh. The value of I_0 is used as a normalizing factor to the following detector signals.

The ULE Ge detector has the following specifications: The active diameter and the thickness of the pure-Ge crystal are 6.2 and 5 mm, respectively. The observed energy resolution is 130.7 eV [full width at half maximum (FWHM)] at 5.9 keV using ⁵⁵Fe and 480.7 eV at 122 keV using ⁵⁷Co. The detector has a specially fabricated multilayer-polymer film vacuum window; the film is supported by a ribbed silicon structure. The film spans silicon ribs that are 100 μm apart and 0.3 mm thick. This ribbed support structure has an 80% open area, that is, parallel “gridded” ribs cover a 20% area of the following vacuum-tight thin film. The total thickness of the film is about 4000 Å covered with a 1400 Å thick aluminum layer. Therefore, the total transmission rate of incident x rays is estimated from the multiplication of the x-ray transmissivity of the polymer film, the aluminum layer, and the open-area ratio of 0.8 of the film.

A current mode is employed for the present calibration. The returning duration τ_{Ge} of the charge-sensitive preamplifier outputs is utilized in this mode. The output signal is automatically returned back (the stored charges in the feedback condenser of the charge-sensitive preamplifier being discharged) to the zero level after reaching a constant preamplifier output level (i.e., a constant comparator voltage level). This mode is useful to obtain an energy response under intensive synchrotron-radiation conditions. Also, a PHA mode is useful not only for cross-checking the above observation method but for identifying higher-harmonic emission levels.

A gold photocathode is mounted in a NIST-type diode with a cylindrical anode.^{12,13} Its electron yield currents I_{Au} are utilized for monitoring photon flux. A photodiode^{14,15} having an 80 Å dead layer (IRD XUV300) is also employed as another I_0 monitor. The output current from each detector is measured with an electropicoammeter and its output voltage is converted into digital pulses with a voltage-to-

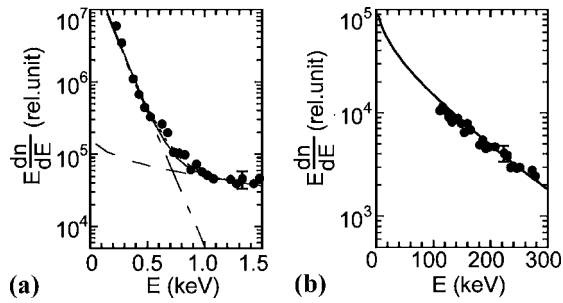


FIG. 3. (a) An x-ray energy spectrum in the central cell obtained by the ULE Ge detector is fitted by the theoretical curve (the solid curve) calculated using two-component Maxwellian electron distribution function. (b) An x-ray spectrum from higher-energy component is also observed by a NaI(Tl) detector.

frequency converter. Finally they are counted by a scaler with 10 s of accumulation and processed by a micro-computer.

The quantum efficiency of the ULE Ge detector normalized by the photon energy, η_{Ge}/E ,¹² is plotted in Fig. 2(b). The curve in Fig. 2(b) shows the results from theoretical calculations using a nominal response curve of the 4000 Å thick polymer window, 1400 Å thick Al layer, and a Ge dead layer. Here, the relative values of the data are normalized to the theoretical curve at $E=0.55$ keV. The experimental results of the normalized detection currents of I_{Ge}/I_0 and I_{Au}/I_0 give the energy response of $I_{\text{Ge}}/I_{\text{Au}}$ for the normalized incident photon flux. I_{Ge} denotes the detection current of the ULE Ge detector. Here, I_{Ge} is proportional to τ_{Ge}^{-1} ; the values of τ_{Ge} without x rays (due to thermal noises) are several orders of magnitude longer than that with x rays. The quantum efficiency of gold, $\text{QE}(E)$, is proportional to the normalized energy response of I_{Au} to the incident photon flux.^{16–18} Therefore the values of η_{Ge} are calculated from $I_{\text{Ge}}/I_{\text{Au}}$ multiplied by $\text{QE}(E)$. The data are cross-checked by using the XUV300 as well.

Although some discrepancies are found near the carbon absorption edge, the data obtained tend to fit the calculated curve. More detailed data fitting could be made if we obtain precise information on the polymer thickness and/or a dead-layer thickness. As the data in Fig. 2(b) show, we may actually expect to investigate plasma x-ray spectra even in a few hundred eV using such an easily handled semiconductor detector in a PHA mode.

IV. EXPERIMENTAL RESULTS

In GAMMA 10 the representative operational modes are characterized in terms of a high potential mode having kilovolt order plasma confining potentials and a hot ion mode yielding deuterium-deuterium fusion produced neutrons with 10–20 keV bulk ion temperatures. Various physics scalings including T_e with ϕ_b in both operational modes are discussed in Refs. 1–3. The present study is carried out in the high potential experimental mode (for more details, see Refs. 1–3).

Figure 3(a) shows an x-ray spectrum from the ULE Ge detector during the period with central ECH. Photons with energy even less than 1 keV are measured by the detector.

Comparing to conventional PHA system such as a Si(Li) detector, the ULE Ge detector shows the benefits of applicability to low-temperature measurements. The dashed-and-dotted and dashed curves are calculated using relativistic Maxwellian distributions with electron temperatures of 125 eV and 3 keV, respectively. Data are well fitted by the dotted curve calculated with bulk electron temperature of 125 eV (99%) along with warm electron temperature of 3 keV (1% to the total density). On the other hand, radial electron temperature profile obtained from x-ray absorption method using the MCP tomography system consistently shows bulk electron temperature $T_e=125\pm 10$ eV at plasma radius $r=0$. Fitting curve for more detailed analysis of the spectrum is obtained as the solid curve in Fig. 3(a) by taking into account the radial profiles of bulk electron temperature and density along the line of sight. The difference between the curve calculated only from the on-axis parameters and one calculated including radial profiles of plasma parameters is less than 8% in the present experiment. In general x rays from core plasma dominantly contribute to x-ray spectra, however, the difference indicates the usefulness and the necessity of the x-ray tomography data when we strictly analyze the x-ray energy spectrum data. By using the ULE Ge detector, x-ray spectrum from both bulk and warm electron components is observed simultaneously for the first time in GAMMA 10. The spectrum directly gives information on electron temperatures and the ratio of bulk electrons to warm electrons.

Figure 3(b) shows a spectrum from the hot electron component obtained by the NaI(Tl) detector. Data are well fitted by the solid curve calculated using relativistic Maxwellian electron distribution function with temperature of 100 keV. This hot electron component is estimated to be less than 0.1% to the total density and therefore the contribution of the hot component as an electron heating source is negligible compared to other terms.

¹T. Cho *et al.*, Phys. Rev. Lett. **64**, 1373 (1990).

²T. Cho *et al.*, Phys. Rev. Lett. **86**, 4310 (2001).

³T. Cho *et al.*, Phys. Rev. Lett. **94**, 085002 (2005).

⁴T. Cho *et al.*, Nucl. Fusion **41**, 1161 (2001).

⁵T. Cho *et al.*, Nucl. Fusion **43**, 293 (2003).

⁶T. Cho *et al.*, Phys. Rev. A **45**, 2532 (1992).

⁷J. Kohagura *et al.*, Rev. Sci. Instrum. **66**, 2317 (1995).

⁸M. Hirata *et al.*, Nucl. Instrum. Methods Phys. Res. B **66**, 479 (1992).

⁹J. Kohagura *et al.*, Rev. Sci. Instrum. **75**, 3992 (2004).

¹⁰N. Saito, I. Suzuki, H. Onuki, and M. Nishi, Rev. Sci. Instrum. **60**, 2190 (1989).

¹¹T. Saito, Metrologia **40**, S159 (2003).

¹²T. Cho, N. Yamaguchi, T. Kondoh, M. Hirata, S. Miyoshi, S. Aoki, H. Maezawa, and M. Nomura, Rev. Sci. Instrum. **59**, 2453 (1988); **60**, 2337 (1989).

¹³T. Kondoh, N. Yamaguchi, T. Cho, M. Hirata, S. Miyoshi, S. Aoki, H. Maezawa, and M. Nomura, Rev. Sci. Instrum. **59**, 252 (1988).

¹⁴J. Kohagura, M. Hirata, T. Tamano, K. Yatsu, and S. Miyoshi, Phys. Rev. E **56**, 5884 (1997).

¹⁵J. Kohagura *et al.*, Nucl. Instrum. Methods Phys. Res. A **477**, 215 (2002).

¹⁶R. H. Day, P. Lee, E. B. Saloman, and D. J. Nagel, J. Appl. Phys. **52**, 6965 (1981).

¹⁷B. L. Henke, J. A. Smith, and D. T. Attwood, J. Appl. Phys. **48**, 1852 (1977).

¹⁸B. L. Henke, J. P. Knauer, and K. Premaratne, J. Appl. Phys. **52**, 1509 (1981).

Review of Scientific Instruments is copyrighted by the American Institute of Physics (AIP). Redistribution of journal material is subject to the AIP online journal license and/or AIP copyright. For more information, see <http://ojps.aip.org/rsio/rsicr.jsp>